SPECTROSCOPY OF COMET P/SCHAUMASSE

NEAL JAMES JOUNG TURNER and GRAEME H. SMITH
University of California Observatories/Lick Observatory, and Board of Studies in Astronomy & Astrophysics, University of California, Santa Cruz, CA 95064, USA

(Received June 15, 1995)

Abstract. Column density profiles for CN, C_3, C_2 and NH have been determined from a long-slit CCD spectrum of periodic comet P/Schaumasse (1992x). Comparisons of these profiles with Haser models indicate that the ratios of the CN, C_3 and C_2 production rates are typical for a short-period comet. Although the scale lengths for NH and its parent species are uncertain, the results indicate that the production rate for NH is much greater than for either C_2 or CN.

Key words: Comets: spectroscopy

1. Introduction

Comet P/Schaumasse is a short-period comet discovered in 1911. Its orbit has a period of 8.2 years, a semi-major axis of 4.07 AU, and an eccentricity of 0.70 (IAU Circular 5666, 1992). Although P/Schaumasse has made ten returns to perihelion since discovery, only limited spectroscopy of it is reported in the literature. For example, it is represented by two low-dispersion objective prism spectra in the Atlas of Representative Cometary Spectra (Swings and Haser, 1956). Spectroscopy obtained during the 1984–85 perihelion approach is discussed by Cochran *et al.* (1992). Difficulties in the recovery of this comet on several perihelion passages may account for the limited spectroscopic coverage prior to 1984. P/Schaumasse does not appear to have been sighted during the 1935 and 1968 returns to perihelion (Marsden, 1969; Cronk, 1984), while during the 1976 return it was recorded on only a single photographic plate, taken by Roemer (Comet News Service 1984). Positional observations made on several other returns indicate that the motion of P/Schaumasse is subject to substantial non-gravitational effects (Marsden, 1968, 1969). These may have contributed to the difficulties in recovery on some returns.

The 1993 perihelion approach of P/Schaumasse was favorable for observation. Imaging of the coma during the period February 22–24 through filters that isolate emission in the C_2 $\Delta v = 0$ band is described by Rousselot *et al.* (1995). Their images reveal an isotropic coma with no indication of any jets. P/Schaumasse (1992x) reached perihelion on 1993 March 4. A spectrum of its coma was obtained ten days later by Churyumov *et al.* (1994).

This paper describes long-slit spectroscopy of P/Schaumasse (1992x) carried out 18 days before the 1993 return to perihelion. The data have been used to derive column-density profiles across the coma for the species NH, CN, C_3 and C_2. Comparisons with theoretical profiles based on Haser models are described for

Earth, Moon and Planets **73:** 33–50, 1996.

each of these four species, and production rates derived from these comparisons are presented.

2. Observations

A long-slit spectrum of Comet P/Schaumasse (1992x) was obtained during twilight on the evening of 13 February 1993 Pacific Standard Time (PST). The KAST spectrograph was used on the Shane 3.0-m telescope at Lick Observatory (Miller and Stone, 1993). At the time of observation the comet was 1.225 AU from the Sun and 0.547 AU from Earth (IAUC No. 5666).

The slit of the spectrograph was oriented north-south and its width was set to 1.5″. A 452 g/mm grism was used in conjunction with a 1200 × 400 pixel Reticon CCD to produce a two-dimensional spectrum having a dispersion of 1.8 Å/pixel and an image scale perpendicular to the dispersion direction of 0.78″/pixel. The pixel scale along the slit direction is such that at the time of observation of P/Schaumasse, 309 km at the comet projected to one pixel on the detector. The useful area of the CCD was 1200 × 160 pixels, which covers the wavelength range 3100–5190 Å and spans the full length of the slit on the sky (2.08′).

The brightest part of the coma was centered on the spectrograph slit by eye. The exposed CCD frame consists of parallel spectra that are dispersed along the CCD rows. These spectra give the intensity distribution across the coma, as a function of wavelength, along a north-south line extending to angular displacements of 1′ from the nucleus. The duration of the comet observation was 300 seconds. The exposure was begun at PST 18 : 42 February 13 (UT 02 : 42 February 14), at which time the hour angle of P/Schaumasse was 0 : 00. The comet observations were followed by exposures of an arc lamp and a flux standard star. A twilight sky frame that was used in the data reductions was obtained during the following evening (PST February 14). The sky exposure was commenced at a Pacific Standard Time similar to that at which the comet observation had begun. The telescope was pointed at an hour angle of 0:05 and a declination corresponding to that of comet P/Schaumasse on the previous night.

The data were reduced using the IRAF software package.* A baseline was subtracted from each CCD frame, this being obtained by fitting a linear spline function to the single overscan column included with each frame.

The CCD frame containing the comet spectra was flat-fielded by dividing it by the median of seven exposures of an illuminated region on the inside of the 3.0-m dome. In order to remove from the flat-field frame the larger-scale spectral energy distribution of the lamp used to illuminate the dome, the medianed flat-field frame was first smoothed with a two-dimensional Gaussian having a σ of 20

* IRAF is distributed by the National Optical Astronomy Observatories, which is operated by the Association of Universities for Research in Astronomy, Inc., under contract to the National Science Foundation.

pixels in the dispersion direction and 3 pixels in the perpendicular direction. This smoothed frame was then divided into the original, thereby producing a normalised flat-field frame that was employed in the reduction of the comet spectra. Use of the smoothing function reduced the usable wavelength range of the data by about 35 Å.

Cosmic rays were selected by inspection of both the flat-field and comet frames. They were removed by interpolating across the affected pixels using the IRAF task fixpix.

Wavelength calibration of the comet frame was derived from an exposure of a HgCdHeAr comparison lamp that was commenced 16 minutes after the end of the comet observation. Dispersion solutions employing fifth-order polynomials were fitted to the arc spectra along every tenth row of the CCD comparison frame. The resulting one-dimensional functions were interpolated into a two-dimensional dispersion function, which was applied across the comet frame.

A flux calibration was applied to each row of the comet frame. This calibration was determined from a 180 second observation of the flux standard star Feige 15, with a wavelength dependence based on the standard KPNO extinction curve included with IRAF. The observation of Feige 15 was started 23 minutes after the conclusion of the comet exposure, when the hour angle of the star was +02 : 51. The wavelength-calibrated and extinction-corrected spectrum of Feige 15 was compared with the known flux of this star in 34 wavelength bins, and a sensitivity function derived, which was then applied to each row of the reduced comet frame.

The flux standard star was observed through the same 1.5″ wide spectrograph slit as the comet. The full width at half-maximum intensity (FWHM) of the recorded spectrum of Feige 15 was measured to be 3.5″ in the direction perpendicular to the dispersion, at wavelengths longward of 3800 Å. If the seeing disk of Feige 15 during the observation was of this size then significant light loss would have occurred at the slit. Assuming that the radial intensity distribution in the seeing disk of the star can be represented by a Gaussian function, and that the star was precisely centered on the slit throughout the observation, the fraction of light lost at the slit is calculated to be ≈60%.

3. Results

3.1. THE INTEGRATED SPECTRUM

The flux-calibrated, wavelength-calibrated, sky-subtracted CCD frame was summed along the slit direction to produce the integrated spectrum of comet P/Schaumasse plotted in Figure 1. This spectrum shows the molecular features typical of a comet at a heliocentric distance slightly greater than 1.0 AU. The λ3135 OH band is apparent near the violet end of the spectrum, but the data do not extend sufficiently far into the ultraviolet to reveal the stronger λ3085 OH band. Similarly, the spectrum records the λ4735 $\Delta v = +1$ C_2 band, but does not extend sufficiently redward

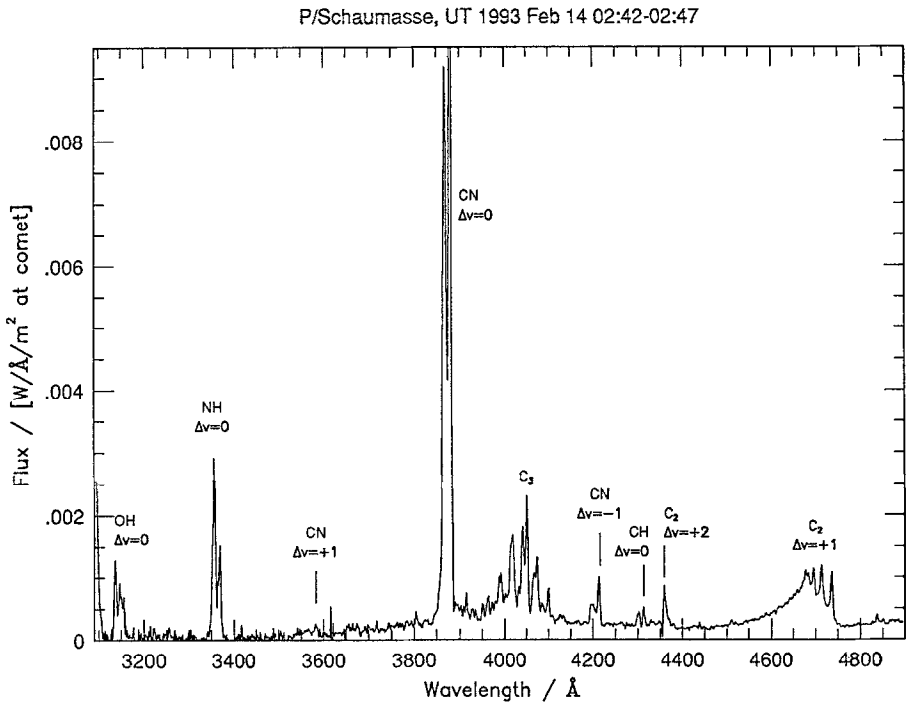

Figure 1. Spectrum of the coma of comet P/Schaumasse, integrated along a 2.1′ north-south slit. The spectrum is the result of a 300 second exposure, and was obtained using the KAST spectrograph on the Lick Observatory 3.0-m telescope.

to reveal all of the stronger $\Delta v = 0$ band. Since only part of this band falls on the CCD, it is not plotted in Figure 1. The $\lambda 3883$ $\Delta v = 0$ CN band is the most prominent feature in the spectrum. The $\Delta v = -1$ CN band at $\lambda 4215$ is also visible, and the location of the $\Delta v = +1$ band is also shown, though it is debatable whether this band is visible in the data. The spectrum also exhibits a prominent $\lambda 3360$ NH band. This band has not often been recorded in ground-based spectra of comets, which generally have not extended as far into the ultraviolet as the spectrum in Figure 1.

3.2. Flux profiles

For each row in the reduced CCD frame, the integrated fluxes in the $\lambda 3360$ NH, $\lambda 3883$ $\Delta v = 0$ CN, $\lambda 4050$ C_3 and $\lambda 4735$ $\Delta v = +1$ C_2 bands have been calculated by summing the flux across each band according to the formula

$$F = \sum_{\lambda_1}^{\lambda_2} F_\lambda - N_p F_c, \tag{1}$$

Table I

Wavelength ranges of molecular emission bands and adjacent continuum regions

Band	Wavelength range/Å
NH $\Delta v = 0$	3339–3382
Continuum	3700–3815
CN $\Delta v = 0$	3830–3905
Continuum	3910–3970
Continuum	3910–3970
C_3 $\Delta v = 0$	3975–4150
Continuum	4155–4190
Continuum	4426–4505
C_2 $\Delta v = +1$	4550–4750
Continuum	4752–4833

where F denotes the total flux in one row of the CCD frame in an emission band that covers the wavelength range from λ_1 to λ_2, F_λ is the flux recorded in the pixel corresponding to wavelength λ, N_p is the number of pixels between λ_1 and λ_2, and F_c is the average flux per pixel in the continuous spectrum over the wavelength range λ_1 to λ_2. The wavelength ranges over which molecular emission was summed are listed in Table I. In the case of the CN and C_3 bands these wavelength regions are the same as those used by Schulz *et al.* (1994), while for the NH and C_2 bands they were chosen so as to include all of the emission evident in Figure 1. For the CN, C_3 and C_2 emission features, the average continuum flux F_c was estimated for each row of the CCD frame by linear interpolation between the fluxes in continuum regions whose wavelength ranges are also listed in Table I. For the NH emission band the nearby continuum is close to zero and is also noisy, as Figure 1 shows, so no continuum subtraction was performed. The integrated emission-band fluxes are plotted in Figure 2 versus projected angular distance from the photocenter of the coma.

3.3. Column Density Profiles

The flux profiles shown in Figure 2 can be converted to column density profiles according to the following formalism. Each row in the two-dimensional spectrum of the coma of P/Schaumasse subtends a solid angle Ω on the sky that is 1.5″ (the width of the spectrograph slit) by 0.78″ (the CCD pixel scale at the KAST spectrograph), i.e., $\Omega = 1.17$ square arc seconds. This in turn corresponds to a projected area at the comet of $A = \Omega R^2 = 1.84 \times 10^5$ km^2, where R (=0.547 AU) is the distance between the Earth and the comet at the time of the observation,

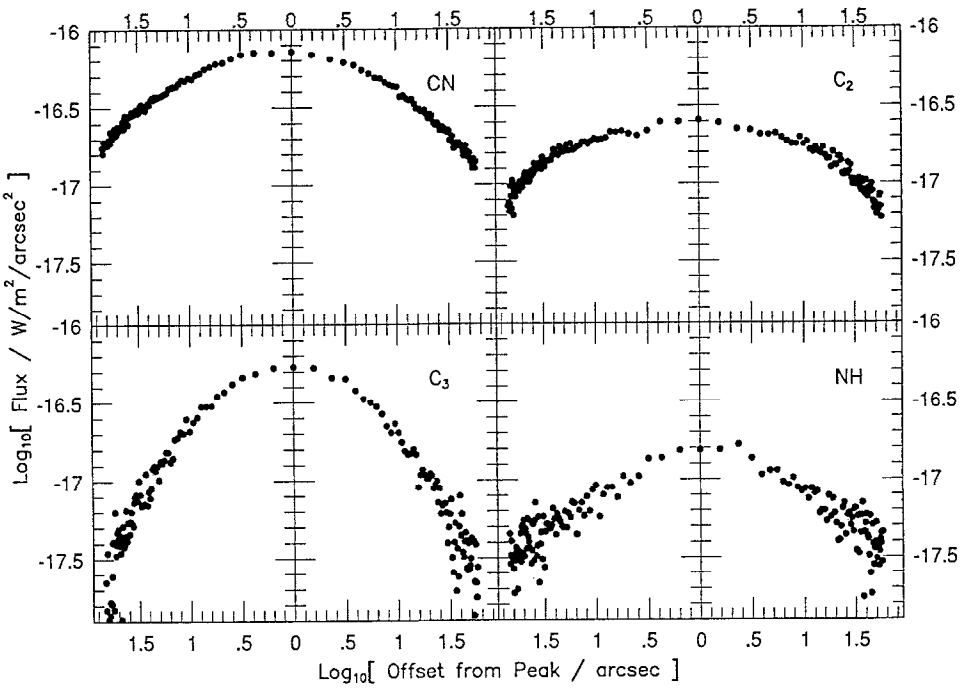

Figure 2. Flux profiles across the coma of P/Schaumasse are shown for the λ3883 CN, λ4735 C_2, λ4050 C_3 and λ3360 NH emission bands. The fluxes are expressed in units of Watts per square meter of collecting area per square arc second field of view.

and Ω is in units of steradians. The total number of molecules N in the coma of P/Schaumasse within the column of projected area A is

$$N = nA = n\Omega R^2, \tag{2}$$

where n is the column density through the coma along the line of sight. For an ensemble of N molecules, the rate of energy emission L (in Watts) is given by the equation

$$L = gN, \tag{3}$$

where g is the rate of energy emission per molecule (in Watts/molecule), and is known as the fluorescence efficiency. Each molecule in the coma is taken to emit radiation isotropically, so that if F is the observed flux from a specific column through the coma (in units of Joules/m^2/s), then the total luminosity due to all of the molecules within this column is

$$L = 4\pi R^2 F. \tag{4}$$

Substituting Equations (3) and (4) into Equation (2) gives the relationship between the column density along a line of sight through the coma and the flux received by an observer

$$n = \frac{4\pi}{g}\frac{F}{\Omega}. \tag{5}$$

The factor $g/4\pi$ that appears in this equation is the fluorescence efficiency per steradian, i.e., the amount of energy emitted per second by a molecule into a solid angle of one steradian.

The value of g to be used in Equation (5) depends on the molecular band that is observed. Both the C_3 and C_2 band efficiencies were assumed to vary as the inverse square of the heliocentric distance of the comet. In the case of the λ4050 C_3 band, the fluorescence efficiency was computed from an equation given by Newburn and Spinrad (1989). Since not all of the C_2 $\Delta v = 0$ band at λ5165 is included in the Lick 3.0-m spectrum, the analysis of the C_2 column density is based on the flux in the λ4735 $\Delta v = +1$ band. For this band, Sivaraman *et al.* (1987) quote a g value of 2.4×10^{-20} Watts/molecule at a heliocentric distance of $r = 1$ AU, implying $g = 1.60 \times 10^{-20}$ Watts/molecule at $r = 1.225$ AU. A similar value, 1.65×10^{-20} Watts/molecule, is obtained by using the formula of Newburn and Spinrad (1989) for the λ5165 $\Delta v = 0$ band efficiency, and scaling the result according to a constant flux ratio among the C_2 bands (A'Hearn, 1975) of C_2 (λ4735)/C_2(λ5165) = 0.55 (A'Hearn, 1978).

In the case of CN and NH bands, the fluorescence efficiency depends on both the heliocentric distance of a comet, r, and the radial velocity, v_r, which was calculated from the equation (Krishna Swamy, 1986)

$$v_r = \pm\sqrt{GM_\odot \frac{a^2e^2 - (a-r)^2}{ar^2}}, \tag{6}$$

where G is the universal gravitational constant, $M_\odot$ is the mass of the Sun, a is the semi-major axis of the comet's orbit, and e is the eccentricity of the orbit. For P/Schaumasse at the time of observation, $r = 1.225$ AU and $v_r = -4.35$ km/s. The g value for the λ3360 $\Delta v = 0$ NH band was read from Figure 3 of Kim *et al.* (1989) and converted to a heliocentric distance appropriate to the P/Schaumasse observation. The fluorescence efficiency for the λ3883 $\Delta v = 0$ CN band was obtained from the grid of values of $F/(n\Omega) = g/(4\pi)$ computed by Tatum (1984).

The resulting g values used in this work are listed in Table II. The column density profiles derived using these g values are shown in Figure 3.

3.4. PRODUCTION RATES

The column density profiles in Figure 3 can be used to calculate production rates within the context of the Haser (1957) model. In this model, non-emitting parent

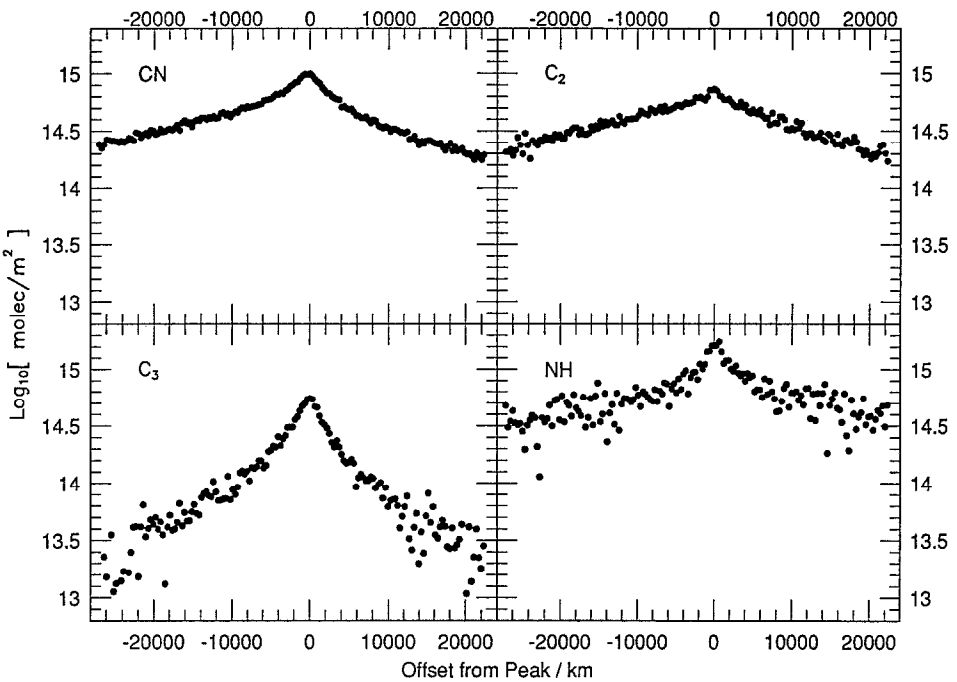

Figure 3. Column density profiles for CN, C_2, C_3, and NH, calculated from the flux profiles shown in Figure 2. The g values used in the calculations are listed in Table II.

Table II

Fluorescence efficiencies for $r = 1.225$ AU and $v_r = -4.35$ km s^{-1}

Species	Wavelength range/Å	Transition	Fluorescence efficiency g W/molecule
NH	3339–3382	$\Delta v = 0$	4.3×10^{-21}
CN	3830–3905	$\Delta v = 0$	3.3×10^{-20}
C_3	3975–4150	$\Delta v = 0$	6.7×10^{-19}
C_2	4550–4750	$\Delta v = +1$	1.6×10^{-20}

species released from the comet nucleus move radially outward at uniform speed and break down to form the emitting species, which then also break down. While the model does not accurately represent the physics of the coma, it is useful as an empirical tool for estimating the rates of gas production at the nucleus. According to the model, the density of an emitting species in the coma varies with radius as

$$n(R) = \frac{Q}{4\pi v}\frac{\beta_0}{\beta_1 - \beta_0}\frac{1}{R^2}(e^{-\beta_0 R} - e^{-\beta_1 R}), \tag{7}$$

where Q is the molecule production rate, v is the radial outflow speed of the molecules, and β_0 and β_1 are the inverses of the scale lengths for breakdown of

the parent and emitting species respectively. The density distribution in this model is spherically symmetric. The column density $N(\rho)$ along a line of sight having a projected distance ρ from the photocenter is given by integrating $n(R)$ along this line:

$$\begin{aligned} N(\rho) &= 2\int_0^\infty n(R)\,dz \\ &= \frac{Q}{2\pi v}\frac{\beta_0}{\beta_1-\beta_0}\int_0^\infty \frac{1}{\rho^2+z^2}(e^{-\beta_0\sqrt{\rho^2+z^2}} - e^{-\beta_1\sqrt{\rho^2+z^2}})dz, \end{aligned} \tag{8}$$

where z denotes distance along the line of sight, and $R^2 = z^2 + \rho^2$. This equation can be rewritten using the substitution $y = z/\rho$ to give

$$\begin{aligned} N(\rho) &= \frac{Q}{2\pi v}\frac{\beta_0}{\beta_1-\beta_0}\int_0^\infty \frac{1}{1+y^2}(e^{-\beta_0\rho\sqrt{1+y^2}} - e^{-\beta_1\rho\sqrt{1+y^2}})dy, \\ &= \frac{Q}{2\pi v}A(\rho). \end{aligned} \tag{9}$$

Equivalent expressions for $A(\rho)$ in terms of second-order modified Bessel functions are discussed by Haser (1957) and O'Dell and Osterbrock (1962).

The integral $A(\rho)$ was evaluated numerically over a range of projected distances ρ matching the extent of the spectrograph slit. Figure 4 illustrates $A(\rho)$ versus ρ for the CN radical. The adopted scale lengths for the parent and emitting species respectively are $1/\beta_0 = 20\,000$ km (see below) and $1/\beta_1 = 6.3 \times 10^5$ km (Newburn and Spinrad, 1989). Also shown is the mean CN column density profile for P/Schaumasse, obtained by averaging the two profiles measured on either side of the nucleus. The solid curve corresponding to $A(\rho)$ has been shifted vertically to superimpose it on the observed column densities.

The logarithmic ordinate in Figure 4 emphasizes the mismatch close to the nucleus between the Haser model and the observed column density. This mismatch is likely caused by one or more of the following: the lack of allowance in the model calculation for the non-zero width of the spectrograph slit; atmospheric seeing; an offset between the slit and the true brightness peak of the coma; and the breakdown of the Haser description near the nucleus. To determine how large an offset between slit and photocenter is required to produce the observed mismatch, Haser profiles modified by offsets of 1, 2 and 3″ were calculated; $A(\rho)$ was resampled as $A(\sqrt{D^2+\rho'^2})$, where D is the offset and ρ' is the distance along the slit from the location of maximum observed brightness, which now is displaced from the true photocenter. All models were matched to the outer parts of the observed column density profile. In Figure 4, the innermost region of the observed profile lies between the curves for $D = 1''$ and $D = 2''$, suggesting that any offset is of the same order as the slit width and the seeing, and less than 2″. For the CN

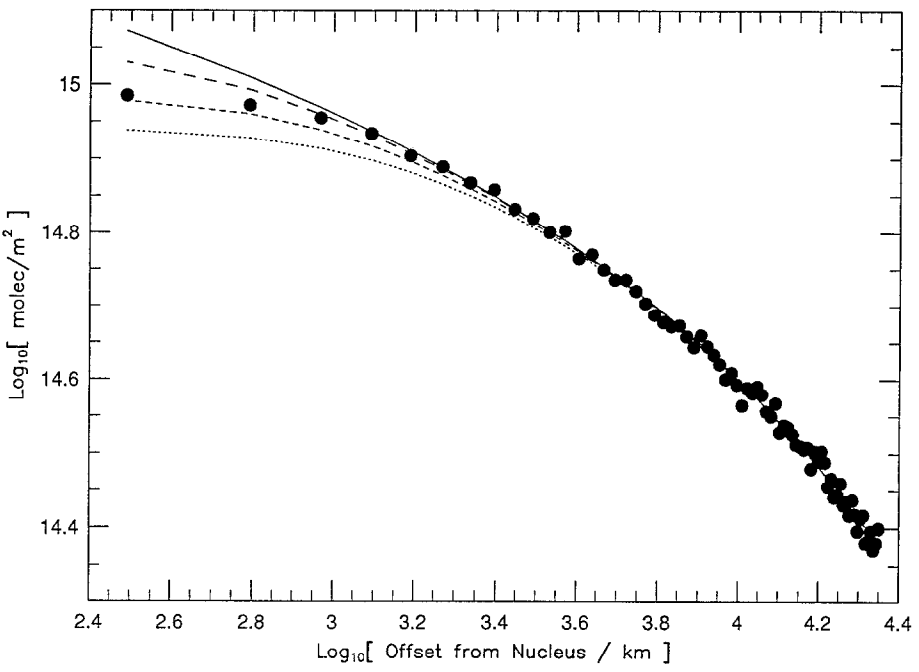

Figure 4. The CN column density profile (dots) of P/Schaumasse superposed on profiles calculated from a Haser model (lines). The CN column densities plotted in this figure are averages between the data to the north and south of the coma center in Figure 3. The long-dashed, short-dashed and dotted lines show the same Haser model as seen with offsets between a spectrograph slit and the photocenter of 1″, 2″ and 3″, respectively. The scale lengths used in the Haser model are 20 000 km for the parent species and 6.3×10^5 km for the emitting CN radical.

radical, the mismatch of the Haser model is negligible outside of 1000 km from the location of the peak in the observed column density profile.

Production rates were derived from plots of the ratio between the observed column density $N(\rho)$ and the Haser model term $A(\rho)$. The relation used is

$$\log\left(\frac{Q}{2\pi v}\right) = \log N(\rho) - \log A(\rho), \tag{10}$$

and the outflow speed in the coma is assumed to be $v = 1$ km s^{-1}. To evaluate $A(\rho)$, values must be adopted for the parent and emitting-species scale lengths β_0 and β_1. A summary of published CN, C_3, C_2 and NH scale lengths currently in use is given in Table III. The scale length values adopted to match the P/Schaumasse observations are listed in Table IV, along with the corresponding production rates.

3.4.1. *The CN Production Rate*

Figure 5 shows a plot of log $N(\rho)$ − log $A(\rho)$ (left-hand axis) versus projected cometocentric distance for the CN radical. A corresponding scale of values for log

Table III

Published values for Haser model scale lengths, in units of 1000 km, and for a heliocentric distance of $r = 1$ AU. Below the heading for each species, the parent scale length is listed on the left and the emitting-species scale length is on the right

Reference	CN		C_3		C_2		NH	
	1000 km		1000 km		1000 km		1000 km	
Newburn and Spinrad (1989)	18	420	3.0	100	31	120	–	–
Cochran (1985)	17	300	3.1	150	25	120	–	–
A'Hearn (1982)	22	300	1	60	17	120	–	–
Schleicher and Millis (1989)	16	300	1	60	16	110	50	100
Combi (1978)	–	–	–	–	–	–	5.8	430

Table IV

Haser model scale lengths used in this paper (columns 2–5), with corresponding production rates for an assumed gas outflow speed of $v = 1$ km s^{-1} (column 6). In column 7, production rates are given for an outflow speed of $v = 0.5$ km s^{-1}, and a 60% light loss at the slit during the observation of the flux standard star. Scale lengths are in units of 1000 km, and are assumed to vary with heliocentric distance as r^2. Comet P/Schaumasse was 1.225 AU from the Sun at the time of observation

Species	$r = 1$ AU		$r = 1.225$ AU		Production rate Q	Corrected production
	Parent 1000 km	Emitting 1000 km	Parent 1000 km	Emitting 1000 km	molecules/s	rate
CN	13	420	20	630	2.9×10^{25}	6.1×10^{24}
C_3	2.3	100	3.5	150	4.3×10^{24}	9.0×10^{23}
C_2	25	120	38	180	4.4×10^{25}	9.2×10^{24}
NH	50	100	75	150	1.5×10^{26}	3.1×10^{25}

Q_{CN} is shown along the right-hand axis assuming an outflow speed of $v = 1$ km s^{-1}. The three sets of points correspond to three different values for the parent scale length. For CN production in a comet at $r = 1.225$ AU, the results of Newburn and Spinrad (1989) indicate that the parent scale length should be close to $1/\beta_0 =$ 27 000 km, and that the scale length of the emitting species is $1/\beta_1 = 6.3 \times 10^5$ km. In the case of CN the emitting-species scale length is much longer than the range of projected radii covered by the spectrograph slit, so that its exact value has little effect on the Haser model fit. For example, the value of $1/\beta_1$ given by Cochran (1985), which is almost 30% smaller than that of Newburn and Spinrad (1989), yields a fit different by less than 0.01 dex or 3% at all plotted radii. The value given by Newburn and Spinrad (1989) is therefore adopted for all CN profiles shown. As Figure 5 indicates, the measurement of Q_{CN} is somewhat sensitive to the value of the parent scale length. Computations were made for different values of β_0 in order to identify the Haser model for which the right-hand side of Equation (10) is independent of radius, corresponding to a production rate that does not vary

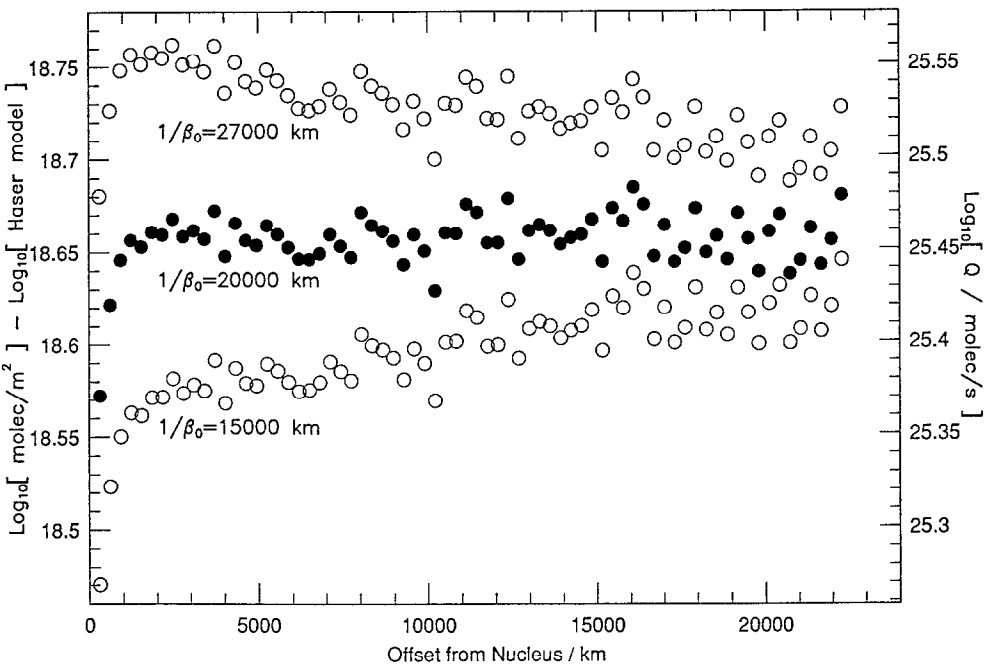

Figure 5. The logarithm of the ratio of observed CN column density to $A(\rho)$ is shown plotted versus projected radius ρ for three different Haser models. The quantity $A(\rho)$ is defined in Equation (9). The three models have parent scale lengths of 27 000, 20 000 and 15 000 km. All have an emitting-species scale length of 6.3×10^5 km.The right-hand axis gives the corresponding production rate, assuming a radial outflow speed for the CN radicals of 1 km s^{-1}. The model plotted with solid dots ($1/\beta_0$ = 20 000 km) was used to calculate the production rate listed in Table IV.

with time. The parent scale length which gives a consistent value of Q_{CN} over the cometocentric radius range sampled by the data is $1/\beta_0$ = 20 000 km, which implies a CN production rate of $Q_{CN} = 2.9 \times 10^{25}$ radicals per second. If the parent scale length were 30% longer than the value adopted here, and equal to the mean found by Newburn and Spinrad (1989) for other comets, the derived value of Q_{CN} would be higher by 20%.

3.4.2. C_3 *Production Rate*

As Figure 6 demonstrates, the derived C_3 column densities at projected radii beyond 10 000 km have a higher dispersion than those closer to the photocenter. Consequently it was decided to base the measurement of Q_{C_3} only on the data for $\rho < 10\ 000$ km. Because the parent scale length of less than 5 000 km is much shorter than the emitting-species scale length of 1.5×10^5 km (Newburn and Spinrad 1989), model fits within 10 000 km of the photocenter are sensitive largely to the parent scale length. The Newburn and Spinrad (1989) value for the emitting-species scale length (at r = 1.225 AU) was therefore adopted in all of the model fits shown in Figure 6. Based on the data in this figure, the appropriate C_3

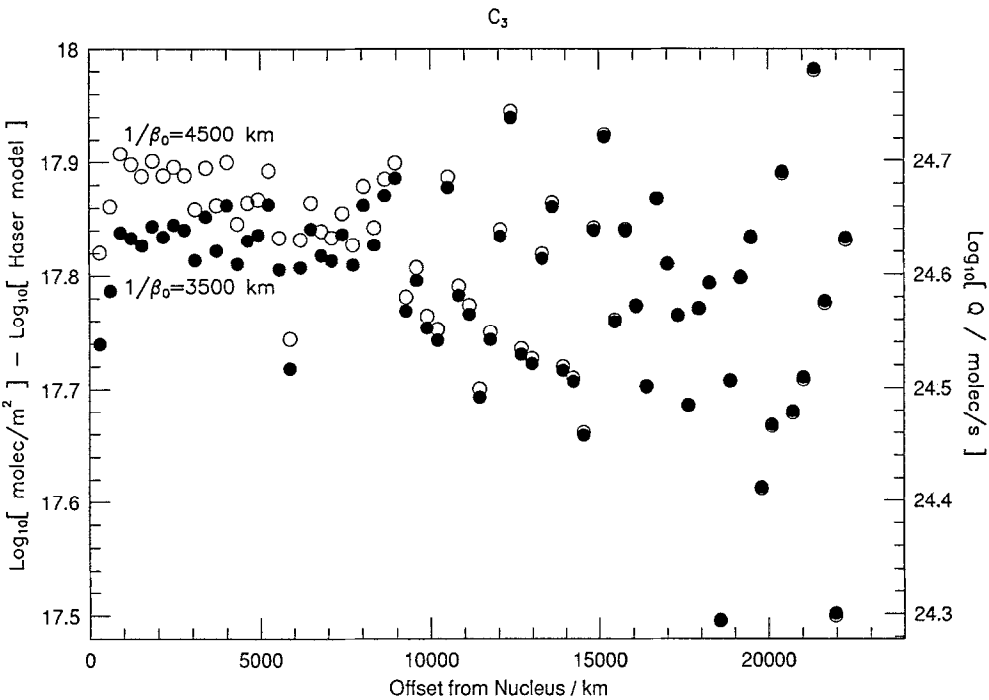

Figure 6. Haser model fits to the column density profile for the C_3 molecule. Both Haser models have an emitting-species scale length of 1.5×10^5 km. The parent scale lengths are 4 500 km (open circles) and 3 500 km (solid dots). The model with $1/\beta_0$ = 3 500 km was used in calculating the production rate.

parent scale length is 3 500 km for r = 1.225 AU, which is about 20% smaller than the value of 4 500 km calculated from the formula of Newburn and Spinrad (1989).

3.4.3. *C_2 Production Rate*

For C_2, the emitting-species and parent scale lengths are sufficiently similar that Haser models fits to the data are quite sensitive to the values of both parameters. As a consequence, adequate fits can be constructed for different combinations of β_0 and β_1 values, with the different fits yielding different production rate estimates. Three Haser model fits to the C_2 column density profile of P/Schaumasse are shown in Figure 7. They were computed for the sets of β_0 and β_1 values published by Newburn and Spinrad (1989), Cochran (1985) and A'Hearn (1982). For the inner 5 000 km, none of these sets yields a satisfactory Haser model. Outside 5 000 km, Cochran's (1985) scale length values yield a production rate that varies least with radius. As the scale on the right-hand side of Figure 7 indicates, the range in C_2 production rates obtained from the three sets of scale lengths is 0.17 dex.

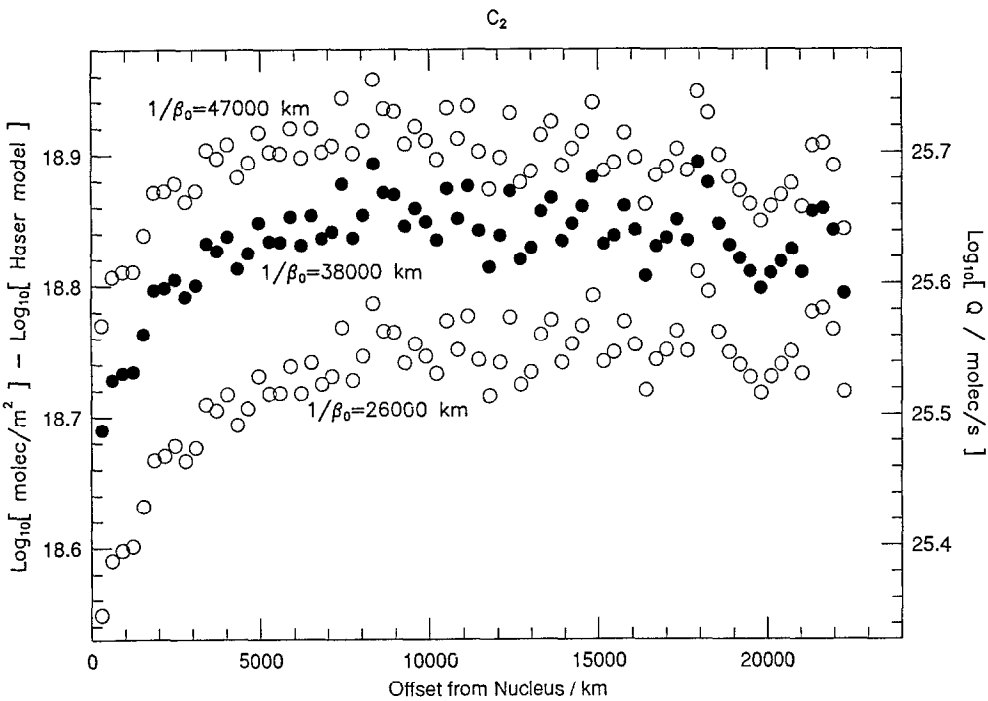

Figure 7. Haser model fits to the column density profile for the C_2 molecule. All three Haser models have an emitting-species scale length of 1.8×10^5 km. The parent scale lengths were taken from Newburn and Spinrad (top set of open circles; 47 000 km), Cochran (1985) (solid dots; 38 000 km) and A'Hearn (1982) (lower set of open circles; 26 000 km). The model with $1/\beta_0 = 38\,000$ km was used to calculate the production rate.

3.4.4. *NH Production Rate*

The scale lengths for cometary NH have not been as extensively studied as those for the other species investigated here. Analyzing the coma of comet Bennett, Combi (1978) determined the parent and emitting-species scale lengths to be 5 800 km and 4.3×10^5 km respectively at $r = 1$ AU, although Kim *et al.* (1989) argued that it is the parent scale length which should be the longer. Schleicher and Millis (1989) examined aperture photometry of P/Halley and found that scale lengths of 50 000 km and 1.0×10^5 km gave a radial variation in the NH production rate that was more consistent with the variations in other species.

Two different sets of NH scale lengths are considered. In the first set, a value in accord with Combi's (1978) result is used for the longer scale length. This length, 4.3×10^5 km at $r = 1$ AU, is again much greater than the largest projected radius

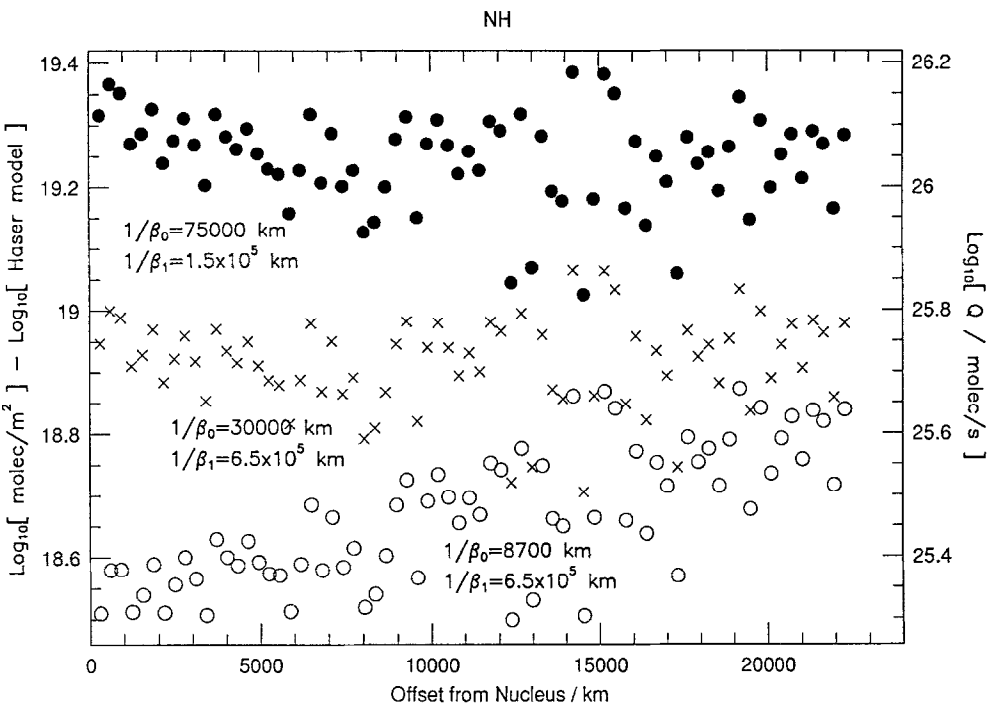

Figure 8. Haser model fits to the column density profile for the NH radical. While the model plotted with solid dots was used to calculate the production rate, the model plotted with crosses provides an equally good fit to the data. It yields a production rate lower by 0.45 dex.

in the available spectrum, so its exact value has only a small effect on the Haser model fit. To match the observed NH column density profile of P/Schaumasse and ensure a radially invariant Q_{NH}, the shorter of the two scale lengths must then be 20 000 km at r = 1 AU, more than three times greater than that determined by Combi (1978) for comet Bennett (Figure 8). The resulting NH production rate is 5.2×10^{25} radicals/second.

The second set of NH scale lengths considered is that found by Schleicher and Millis (1989) for P/Halley. As Figure 8 shows, this set of scale lengths also yields a radially invariant Q_{NH}, but the production rate it predicts is greater by 0.45 dex. The NH production rate is then 1.5×10^{26} radicals/second. Further work is needed to determine which set of NH scale lengths should be preferred.

3.4.5. *Discussion of the Production Rate Measurements*

The CN, C_3 and C_2 production rates derived from the column-density profiles for P/Schaumasse are within the ranges found for other short-period comets by A'Hearn & Millis (1980),* Newburn and Spinrad (1984), and Cochran (1985). The derived production rates are, however, about 1.4 dex larger than rates determined

* The C_3 production rates from A'Hearn and Millis (1980) were revised downwards by Cochran (1987) to take account of revisions in the oscillator strength of the 4050 Å emission band.

by Cochran *et al.* (1992) during 1984 and 1985 when P/Schaumasse was 1.39 to 1.83 AU from the Sun. Part of this difference is due to the use of different values for the gas outflow speed v in the coma. Cochran *et al.* (1992) use the Delsemme (1982) expression $v = (0.58 \text{ km s}^{-1})r^{-1/2}$ to derive the outflow speed, which at r = 1.225 AU leads to gas production rates 0.28 dex lower than are obtained assuming $v = 1 \text{ km s}^{-1}$. In addition, the Cochran *et al.* (1992) observations of P/Schaumasse were obtained when the comet was at larger heliocentric distances than during the present observations. The gas production rates of comets can vary sensitively with heliocentric distance (e.g., Newburn and Spinrad 1989). This effect could account for a difference of up to about 0.3 dex between the production rates in Table IV and those found by Cochran *et al.* (1992).

Errors in the flux calibration of the Lick spectrum of P/Schaumasse also contribute to the difference between the production rates listed in Table IV and those measured by Cochran *et al.* (1992). Such errors are a consequence of light losses at the spectrograph slit during the observation of the flux standard star Feige 15. The use of the resultant Feige 15 spectrum for flux calibration causes the absolute flux in the cometary emission bands to be overestimated. If 60% of the light from Feige 15 was blocked by the slit, as calculated in Section 2, then the column densities and gas production rates given in column 6 of Table IV are 0.4 dex too large. Gas production rates scaled to a molecular outflow speed of $v = 0.5 \text{ km s}^{-1}$, and reduced by 0.4 dex to account for the flux calibration error, are listed in the final column of Table IV. These results are in better agreement with those of Cochran *et al.* (1992), although there is still a systematic difference of $\approx$0.7 dex.

Whereas the absolute gas production rates are sensitive to errors in flux calibration, the ratios between the rates for different species should be more reliably measured. The ratio of the C_3 production rate to that of CN is $Q_{C_3}/Q_{CN} = 0.15$, which is very close to the average value of 0.19 ± 0.13 determined by Cochran (1987) from literature data for a large sample of comets. This is also very similar to a mean value of 0.17 ± 0.06 derived by Cochran *et al.* (1992) from observations of P/Schaumasse made in 1984 September and 1985 February. In calculating a mean Q_{C_3}/Q_{CN} value and standard deviation from the Cochran *et al.* (1992) data, their April 1985 result was not included since it differs greatly from the other 1984–85 measurements. The ratio of the C_2 to CN production rates derived from the Lick spectrum of P/Schaumasse is $Q_{C_2}/Q_{CN} = 1.5$, which is similar to the average of 1.46 ± 0.68 found by Cochran (1987) for a large sample of comets. However, it is greater than the value of 1.08 ± 0.12 calculated from the results of Cochran *et al.* (1992) for P/Schaumasse itself during 1984–85. Since the values of the C_2 scale lengths adopted in this paper are the same as those used by Cochran *et al.* (1992), the difference in the C_2 to CN production ratio hints that P/Schaumasse may have been less active during the 1984–85 perihelion passage than in 1993 February. A difference in activity between the 1984–85 and 1993 passages could also account for some part of the difference between the gas production rates determined by Cochran *et al.* (1992) and those listed in column 7 of Table IV.

4. Summary and Conclusions

A long-slit CCD spectrum of the coma of P/Schaumasse (1992x) has been obtained less than three weeks prior to the 1993 perihelion passage of this comet. The spectrum exhibits prominent emission bands due to CN, C_3, C_2, and NH. Measurements of the emission band fluxes have been used to derive radial column density profiles for these species. Consistent with the results of Rousselot *et al.* (1995), the profiles appear to be smooth, with no evidence for jets.

Haser models have been calculated and fitted to the observed column density profiles. The fit to the profile for the CN radical places an upper limit of 2″ on any displacement of the spectrograph slit with respect to the photocenter of the coma. Haser models are specified by two scale lengths which parameterise the formation and break-up of a molecule or radical. The values adopted for the scale lengths of CN, C_3, C_2, and NH are listed in Table IV, while Table III summarizes previously-published values. The column density profiles for all four species are poorly matched by Haser models within the inner 1000 km of the coma (Figures 5 through 8). The innermost 5 000 km of the C_2 $\Delta v = +1$ data are also not well-fit by Haser models using any of the previously published sets of scale lengths for this molecule. Beyond 5 000 km from the coma photocenter, reasonable matches of Haser models to the column density profiles of all four species have been found, although some of the scale length values adopted are different from those reported in the literature for other comets.

Production rates have been derived for CN, C_3, C_2, and NH, although the measurements are sensitive to the parent scale lengths chosen, as Figure 5 demonstrates. With the adopted scale lengths, the production ratios Q_{C_3}/Q_{CN} and Q_{C_2}/Q_{CN} derived from the Lick data are close to the averages observed among other short-period comets (Section 3.4.5). However, comparison of the Lick observations with measurements made by Cochran *et al.* (1992) in 1984 and 1985 suggests that the C_2/CN production ratio of P/Schaumasse may have differed between the 1984–85 and 1993 perihelion passages, with the ratio during the earlier passage being slightly below the average for other comets.

Acknowledgements

The authors thank Jim Burrous for his expert help in making the observations, and Beth Hufnagel and Scott Trager for their advice on using IRAF.

References

A'Hearn, M. F.: 1975, *AJ* **80**, 861.
A'Hearn, M. F.: 1978, *ApJ* **219**, 768.
A'Hearn, M. F.: 1982, in L. L. Wilkening (ed.), *Comets*, University of Arizona Press, Tucson, pp. 433–460.

A'Hearn, M. F. and Millis, R. F.: 1980, *AJ* **85**, 1528.
Churyumov, K. I., Kleshchenok, V. V., and Vlasyuk, V. V.: 1994, *Soviet Astronomy Letters* **20**, 621.
Cochran, A.: 1985, *AJ* **90**, 2609.
Cochran, A. L.: 1987, *AJ* **92**, 231.
Cochran, A. L., Barker, E. S., Ramseyer, T. F., and Storrs, A. D.: 1992, *Icarus* **98**, 151.
Combi, M. R.: 1978, *AJ* **83**, 1459.
Comet News Service: 1984, Issue 84-4, St. Louis Science Center, Omaha.
Delsemme, A. H.: 1982, in L. L. Wilkening (ed.), *Comets*, University of Arizona Press, Tucson.
Haser, L.: 1957, *Bull. Acad. R. Sci. Belg.* **43**, 740.
Kim, S. J., A'Hearn, M. F., and Cochran, W. D.: 1989, *Icarus* **77**, 98.
Krishna Swamy, K. S.: 1986, *The Physics of Comets*, World Scientific Publishers, Singapore.
Kronk, G. W.: 1984, *Comets: A Descriptive Catalog*, Enslow Publishers, Hillside.
Marsden, B. G.: 1968, *AJ* **73**, 367.
Marsden, B. G.: 1969, *AJ* **74**, 720.
Miller, J. S. and Stone, R. P. S.: 1993, *Lick Observatory Technical Report No. 66.*
Newburn, R. L. and Spinrad, H.: 1984, *AJ* **89**, 289.
Newburn, R. L. J. and Spinrad, H.: 1989, *AJ* **97**, 552.
O'Dell, C. R. and Osterbrock, D. E.: 1962, *ApJ* **136**, 559.
Rousselot, P., Moreels, G., Clairemidi, J., Goidet-Devel, B., and Boehnhardt, H.: 1995, *Icarus* **114**, 341.
Schleicher, D. G., Bus, S. J., and Osip, D. J.: 1993, *Icarus* **104**, 157.
Schleicher, D. G. and Millis, R. L.: 1989, *ApJ* **339**, 1107.
Schulz, R., McFadden, L. A., Chamberlin, A. B., A'Hearn, M. F., and Schleicher, D. G.: 1994, *Icarus* **109**, 145.
Sivaraman, K. R., Babu, G. S. D., Shylaja, B. S., and Rajamohan, R.: 1987, *A&A* **187**, 543.
Swings, P. and Haser, L.: 1956, *Atlas of Representative Cometary Spectra*, University of Liege Astrophysical Institute, Tech. Rept. AF61 (514)-628.
Tatum, J. B.: 1984, *A&A* **135**, 183.